

# Coherent optical ultrasound detection with rare-earth ion dopants

Jian Wei Tay, Patrick M. Ledingham, and Jevon J. Longdell\*

Jack Dodd Centre, University of Otago, Department of Physics, 730 Cumberland Street, Dunedin, New Zealand

\*Corresponding author: jevon@physics.otago.ac.nz

Received 21 May 2010; revised 5 July 2010; accepted 6 July 2010;  
posted 12 July 2010 (Doc. ID 128761); published 3 August 2010

We describe theoretical and experimental demonstration for optical detection of ultrasound using a spectral hole engraved in cryogenically cooled rare-earth ion-doped solids. Our method utilizes the dispersion effects due to the spectral hole to perform phase-to-amplitude modulation conversion. Like previous approaches using spectral holes, it has the advantage of detection with large *étendue*. The method also has the benefit that high sensitivity can be obtained with moderate absorption contrast for the spectral holes. © 2010 Optical Society of America

OCIS codes: 110.7170, 190.0190, 260.2030.

Ultrasound is widely used in imaging and nondestructive testing. Most of this testing require an ultrasonic transducer in intimate physical contact with the subject. However, the ability to remotely detect ultrasound removes this restriction, allowing a greater variety of applications. A form of remote detection known as air-coupled ultrasound [1] is under active development. However, sensitivity is limited by small coupling between vibrations in the test object and air due to a large impedance mismatch. Remote optical detection uses the fact that light scattered from a vibrating object becomes phase modulated. The challenge of this method is the detection of the phase modulation sidebands on the received light, which in general is highly spatially multimode.

For situations where the received light is in a well-defined spatial mode, heterodyne detection and other forms of interferometry [2,3] lend themselves readily to the task. Quantum-noise-limited performance can be relatively easily obtained [4]. However, in practical applications where the received light has a complex speckle pattern, the interferometric visibility becomes severely affected resulting in low sensitivity.

The ability of an optical system to process light is measured by its *étendue*,  $\mathcal{E} = S\Omega$ , which is the product of the detection surface area  $S$  and the scattering solid angle  $\Omega$ . Adding optics to the system can change both the collection area and the solid angle but, according to the constant brightness theorem, cannot improve the *étendue*. Interferometry suffers from lower sensitivity as the *étendue* is limited to  $\lambda^2$  due to mode-matching requirements [5]. Confocal Fabry–Perot resonators can achieve better with *étendue* of around  $10^{-3}$  sr mm<sup>2</sup> [6,7].

Adaptive imaging techniques based on photorefractive crystals allow much greater *étendue* compared to classical interferometers [8–10]. In these approaches, the photorefractive crystals act as an adaptive beam splitter, which matches the mode of the probe beam travelling through the sample with a local oscillator. Recent advances have demonstrated fast, efficient photorefractive crystals able to operate in the “therapeutic window” [11]. However, the programming speed utilized for imaging demonstrations ( $\tau_{PR} = 100$  ms) are still slow for biological imaging of thick tissue *in vivo*, where speckle decorrelation times are on the order of 0.1 ms [12].

An adaptive detection scheme using rubidium vapor was recently proposed and demonstrated [13]. This scheme has the advantage of shorter writing

times compared to photorefractive crystals. The scheme employs the use of self rotation of polarized light to “program” the hologram in the atomic vapor. However, it is unclear how the sensitivity of the detection relies on the angular dependence of the beams. In [13], near-parallel signal and reference beams were used, which means there is little Doppler broadening of the two-photon transitions. It is unclear how effective the detection will be when the beams are more than a few degrees apart, as Doppler broadening in the hyperfine transitions used will affect the polarization self rotation [14].

The suitability of rare-earth ion-doped crystals as spectral filters to detect ultrasound has recently been demonstrated by Li *et al.* [15]. In that work, the received light was directed through a Tm:YAG crystal that had a spectral hole prepared at the same frequency as one of the modulation sidebands. The sample absorbed the unmodulated light but let the sideband through, allowing it to be measured directly.

Rare-earth-doped crystals used in this manner allow étendue several orders of magnitude higher than can be achieved using other techniques. However, detecting weak ultrasound signals, where the unmodulated component is much larger than the modulated component, using this approach requires large absorption away from the hole, while simultaneously obtaining high transmission through a narrow hole. Although very high contrast spectral filtering has been demonstrated for Pr<sup>3+</sup> [16], the transition of interest in this case is at 606 nm, where laser sources are difficult to obtain. For other dopants with more convenient wavelengths, such as Tm<sup>3+</sup>, shorter hole lifetimes makes this much more difficult.

Here we demonstrate an alternate scheme using the dispersive properties of an engraved spectral hole. Our method utilizes Tm<sup>3+</sup> ions, which have resonance at 793 nm and are able to be probed using diode and other solid state lasers. We demonstrate that high sensitivity can be achieved using sensible hole-burning parameters.

Our technique relies on the steep dispersion of the spectral hole to convert phase modulation into amplitude modulation. By applying a phase shift to the carrier that is different to that of the two sidebands, phase modulation can be transformed efficiently into amplitude modulation. Using the carrier as a local oscillator allows shot-noise-limited detection of this amplitude modulation. The technique has a lot in common with Pound–Drever–Hall laser stabilization [17] to a spectral hole. However, in this case we are deliberately offset a fixed amount from hole center and are measuring the phase modulation rather than the laser frequency.

We now provide the theoretical description of our system. Consider a monochromatic laser beam reflected off the surface of an object vibrating at ultrasonic frequency  $\omega_M$ . The reflected light [18,19] can be described as

$$E_r(t) = E_0 \exp(i\omega_c t) \exp(-iM \times \text{Re}\{\exp(i\omega_M t)\}), \quad (1)$$

where  $\omega_c$  is the optical frequency,  $E_0$  is the amplitude of the electric field, and  $M$  is the (assumed real) modulation index  $M = 4\pi U/\lambda$ , where  $U$  is the amplitude of the ultrasonic displacement and  $\lambda$  is the optical wavelength. For ultrasonic displacements that are small compared to the wavelength of light (i.e.,  $M \ll 1$ ), this becomes

$$E_r(t) = E_0 \left[ -i \frac{M}{2} \exp(-i\omega_M t) + 1 + i \frac{M}{2} \exp(i\omega_M t) \right]. \quad (2)$$

In our experiment, we used the  ${}^3H_6 \rightarrow {}^3H_4$  transition in Tm:YAG, which occurs around 793 nm. The sample used had an inhomogeneous linewidth of around 30 GHz. This large inhomogeneous broadening means we can assume the absorption spectrum is flat, except where the ions have been optically pumped into the metastable (10 ms) shelving state  ${}^3F_4$ , resulting in a spectral hole.

We can assume that the Tm:YAG crystal so prepared has a complex transmission function  $T(\omega)$ . The phasor for the light transmitted through the crystal is therefore given by

$$E_r(t) = E_0 \left[ -i \frac{M}{2} T(-\omega_M) \exp(-i\omega_M t) + T(0) + i \frac{M}{2} T(\omega_M) \exp(i\omega_M t) \right]. \quad (3)$$

The detected photocurrent that results is given by  $I(t) = \eta q / (\hbar \omega_c) (\epsilon_0 c A / 2) E_r(t)^* \cdot E_r(t)$ . Hence, we obtain

$$I(t) = I_0 (1 + M \times \text{Re}\{\beta \times \exp(i\omega_M t)\}), \quad (4)$$

where  $\beta = T(\omega_M)T(0)^* - T(-\omega_M)^*T(0)$ .

To achieve shot-noise-limited sensitivity, two things are required: first, there can be no loss from the sidebands. Second, as described by Eq. (4), the carrier needs to be phase shifted by  $\pi/2$  relative to the mean phase of the two sidebands to transform the phase modulation completely into amplitude modulation. These could be achieved by having broad spectral holes for the sidebands and an absorptive spike, such as that used in [16,20], sitting to one side of the carrier.

Here, we use a simpler absorption profile using a spectral hole offset from the carrier. The complex transmission function for the spectral hole can be modeled by [21,22]

$$T(\omega) = \exp \left[ -\frac{\alpha L}{2} \left( 1 - \frac{\Gamma}{\Gamma - i\Delta} \right) \right], \quad (5)$$

where  $\alpha L$  is the optical depth,  $\Gamma/2\pi$  is the hole linewidth, and  $\Delta$  is the angular frequency offset between the laser frequency and the center of the hole. When the laser frequency is offset from the hole center, broadband detection is obtained as long as the modulation frequency is larger than the hole width.

Our experimental setup is shown in Fig. 1, with the red solid lines indicating the experimental beam path and the blue dashed lines indicating the locking beam path. We used an extended-cavity diode laser operating at 793 nm, frequency stabilized using a hybrid optical and electronic technique [23]. The laser is locked to a spectral hole engraved in the same crystal, providing a narrow spectral filter for the seeding beam. This gives a dramatically narrower Schawlow–Townes linewidth and much reduced sensitivity to current noise. We measured a 30 dB drop in the amount of phase noise around 1 MHz.

To perform ultrasound measurements, the beam frequency is shifted and gated using two acousto-optic modulators (AOMs). The ultrasound pulses were generated using either an electro-optic modulator (EOM) for calibration of the detection system, or a piezoelectric transducer (PZT)-backed mirror operating at 1.11 MHz. The modulated beam is then directed through a rare-earth ion-doped crystal. The sample used was 0.1% Tm<sup>3+</sup>:YAG (Scientific Materials) cryogenically cooled to 2.9 K. The incident beam on the sample had a power of 0.6 mW and a diameter of 1 mm. The beam arriving at the photodetector had a power of 146 μW.

To generate the signal, the output from the photodetector was AC coupled then amplified using a low-noise rf amplifier (Minicircuits ZFL-500LN). The amplified signal was then downconverted by mixing with a local oscillator at the same rf frequency as the applied ultrasound modulation. This was then amplified using a preamplifier with a gain of 100 and a low-pass filter set to a 30 kHz bandwidth before measurement with an oscilloscope.

The properties of the engraved spectral hole are shown in Fig. 2. The (normalized) transmission is measured by sweeping the laser frequency 4 MHz across the hole and is shown in subplot (a). Using Eq. (5), we can fit to the trace to obtain an optical depth  $\alpha L$  of 0.5 and linewidth  $\Gamma/(2\pi)$  of 371 kHz. The phase shift was then calculated using the Kramers–Krönig relations and is shown in Fig. 2(b). For the optical

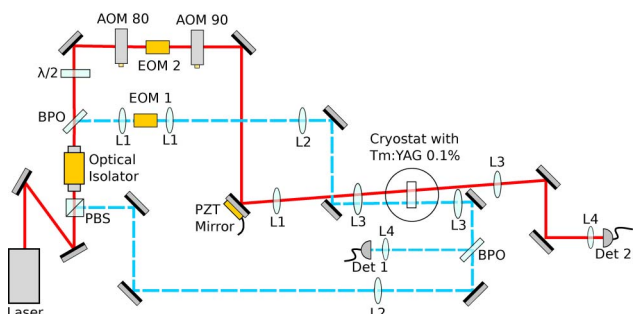


Fig. 1. (Color online) Experimental setup. The experimental beam (path shown by red solid lines) is frequency shifted and gated using two AOMs. The ultrasonic pulses were applied using a PZT-backed mirror. The beam is then steered through a prepared Tm:YAG 0.1% crystal before being detected using a photodetector. The laser is locked to a spectral hole using a method similar to Bottger [22] (path shown by blue dashed lines), except with optical feedback [23].

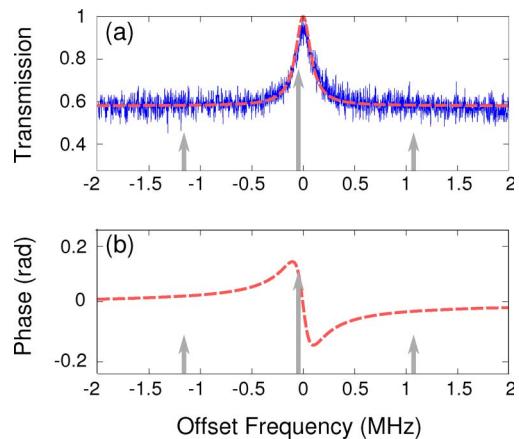


Fig. 2. (Color online) Response of a spectral hole. This shows (a) the normalized transmission through the hole and its calculated fit (calculated fit shown by red dashed curve), and (b) the phase response as given by the Kramers–Krönig relations. The arrows indicate the position of the sideband and carrier frequencies of the ultrasonically modulated light.

depth used, the maximum phase shift obtained is around 0.14 rad, compared to the ideal case of  $\pi/2$ .

We now demonstrate the detection of ultrasound pulses using a spectral hole engraved as before. The laser frequency is shifted by 39 kHz to sit the laser to the side of the spectral hole, as indicated in Fig. 2, to obtain a large phase shift. Ultrasound pulses were then applied using the PZT-backed mirror and the retrieved signal is shown in Fig. 3.

We can calculate the position-equivalent noise on our system from the ratio of detection noise with the sensitivity afforded by the spectral hole. Assuming shot noise and an optimum optical depth such that  $|\beta| = 1$ , the optimal position-equivalent noise for this technique was calculated to be  $1.3 \times 10^{-13}$  m/ $\sqrt{\text{Hz}}$ . However, in practice, the position-equivalent noise on our system was measured to be  $4.6 \times 10^{-11}$  m/ $\sqrt{\text{Hz}}$ , given a 30 kHz detection bandwidth. The reason for increased noise on our detection is twofold: the sample used has a nonoptimum optical depth, leading to reduced phase-to-amplitude conversion, and there is residual phase noise on the laser at ultrasonic frequencies.

In conclusion, we have demonstrated sensitive coherent optical detection of ultrasound using the dispersive properties of spectral holes. The achieved position-equivalent noise is approximately 100 times larger than ideal shot-noise-limited detection. There

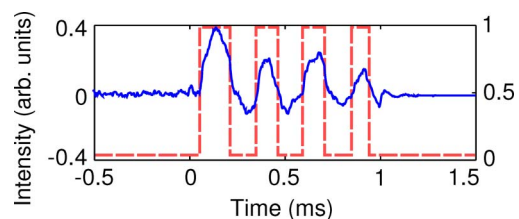


Fig. 3. (Color online) Ultrasonic pulse detection. The detected intensity (blue solid line) is shown with respect to the applied pulses (red dashed line). The axis on the right indicates the normalized pulse amplitude.

are two reasons for this: first, the conversion of phase-to-amplitude modulation with the nonideal spectral hole shape results in a sensitivity one-fifth of the ideal case. Excess noise on the laser above the shot noise level accounts for the rest. The technique is suitable for the optical detection ultrasound with large étendue and, in principle, could reach shot-noise-limited sensitivities with spectral hole-burning materials of modest performance.

This work was produced with the support of the New Zealand Foundation for Research, Science and Technology under contract NERF-UOOX0703.

## References

1. R. Stoessel, N. Krohn, K. Pfeleiderer, and G. Busse, "Air-coupled ultrasound inspection of various materials," *Ultrasonics* **40**, 159–163 (2002).
2. R. J. Dewhurst and Q. Shan, "Optical remote measurement of ultrasound," *Meas. Sci. Technol.* **10**, R139–R168 (1999); and references therein.
3. C. B. Scruby and L. E. Drain, *Laser Ultrasonics* (Adam Hilger, 1990).
4. H.-A. Bachor and T. C. Ralph, *A Guide to Experiments in Quantum Optics* (Wiley-VCH, 2004).
5. A. E. Siegman, "The antenna properties of optical heterodyne receivers," *Appl. Opt.* **5**, 1588–1594 (1966).
6. J.-P. Monchalin, "Optical detection of ultrasound at a distance using a confocal Fabry-Perot interferometer," *Appl. Phys. Lett.* **47**, 14–16 (1985).
7. J.-P. Monchalin, R. Héon, P. Bouchard, and C. Padioleau, "Broadband optical detection of ultrasound by optical sideband stripping with a confocal Fabry," *Appl. Phys. Lett.* **55**, 1612–1614 (1989).
8. R. K. Ing and J.-P. Monchalin, "Broadband optical detection of ultrasound by two-wave mixing in a photorefractive crystal," *Appl. Phys. Lett.* **59**, 3233–3235 (1991).
9. T. W. Murray, L. Sui, G. Maguluri, R. A. Roy, A. Nieva, F. Blonigen, and C. A. DiMarzio, "Detection of ultrasound-modulated photons in diffuse media using the photorefractive effect," *Opt. Lett.* **29**, 2509–2511 (2004).
10. M. Lesaffre, F. Jean, F. Ramaz, A. C. Boccara, M. Gross, P. Delaye, and G. Roosen, "In situ monitoring of the photorefractive response time in a self-adaptive wavefront holography setup developed for acousto-optic imaging," *Opt. Express* **15**, 1030–1042 (2007); and references therein.
11. S. Farahi, G. Montemezzani, A. A. Grabar, J.-P. Huignard, and F. Ramaz, "Photorefractive acousto-optic imaging in thick scattering media at 790 nm with a  $\text{Sn}_2\text{P}_2\text{S}_6:\text{Te}$  crystal," *Opt. Lett.* **35**, 1798–1800 (2010); and references therein.
12. M. Gross, P. Goy, B. C. Forget, M. Atlan, F. Ramaz, A. C. Boccara, and A. K. Dunn, "Heterodyne detection of multiply scattered monochromatic light with a multipixel detector," *Opt. Lett.* **30**, 1357–1359 (2005).
13. N. Korneev, P. Rodríguez-Montero, and O. Benavides, "Rubidium vapor holography for noncontact adaptive detection of ultrasound," *Opt. Lett.* **34**, 1964–1966 (2009).
14. S. M. Rochester, D. S. Hsiung, D. Budker, R. Y. Chiao, D. F. Kimball, and V. V. Yashchuk, "Self-rotation of resonant elliptically polarized light in collision-free rubidium vapor," *Phys. Rev. A* **63**, 043814 (2001).
15. Y. Li, H. Zhang, C. Kim, K. H. Wagner, P. Hemmer, and L. V. Wang, "Pulsed ultrasound-modulated optical tomography using spectral-hole burning as a narrowband spectral filter," *Appl. Phys. Lett.* **93**, 011111 (2008).
16. M. P. Hedges, J. J. Longdell, Y. Li, and M. J. Sellars, "Efficient quantum memory for light," *Nature* **465**, 1052–1056 (2010).
17. R. Drever, J. Hall, F. V. Kowalski, J. Hough, G. M. Ford, A. Munley, and H. Ward, "Laser phase and frequency stabilization using an optical resonator," *Appl. Phys. B* **31**, 97–105 (1983).
18. G. C. Bjorklund, "Frequency-modulation spectroscopy: a new method for measuring weak absorptions and dispersions," *Opt. Lett.* **5**, 15–17 (1980).
19. J. M. Supplee, E. A. Whittaker, and W. Lenth, "Theoretical description of frequency modulation and wavelength modulation spectroscopy," *Appl. Opt.* **33**, 6294–6302 (1994).
20. J. J. Longdell and M. J. Sellars, "Experimental demonstration of quantum-state tomography and qubit-qubit interactions for rare-earth-metal-ion-based solid-state qubits," *Phys. Rev. A* **69**, 032307 (2004).
21. B. Julsgaard, A. Walther, S. Kröll, and L. Rippe, "Understanding laser stabilization using spectral hole burning," *Opt. Express* **15**, 11444–11465 (2007).
22. T. Böttger, "Laser frequency stabilization to spectral hole burning frequency references in erbium-doped crystals: material and device optimization," Ph.D. thesis (Montana State University, 2002).
23. W. Farr, J. W. Tay, P. M. Ledingham, D. Korystov, and J. J. Longdell, "Hybrid optical and electronic laser locking using spectral hole burning" (manuscript in preparation).